

Bond Behavior between Embedded Through-Section Bars and Concrete

Linh Van Hong Bui[#], Boonchai Stitmannaitum[#], Tamon Ueda^{*}, Pitcha Jongvivatsakul[#]

[#]Department of Civil Engineering, Chulalongkorn University, Thailand
E-mail: bvhlinh@gmail.com, Boonchai.S@chula.ac.th (corresponding author), p.jongvivatsakul@gmail.com

^{*}Graduate School of Engineering, Hokkaido University, Japan

Abstract— The embedded through-section (ETS) method has been used as a new technique to strengthen the reinforced concrete beams in shear. In this technique, the fiber-reinforced polymer (FRP) or steel rods are embedded through previously drilled holes into the concrete core. Most of the previous research concluded that the ETS method was proved to be particularly efficient and increase significantly of the shear resistance. This paper focuses on the bond response between the ETS bars and concrete substrate. Three-dimensional (3D) finite element (FE) models of concrete blocks strengthened by ETS bars using ANSYS 15.0 are built and considered. Furthermore, the analytical formulation of the slip profiles is offered to assess the bond performances of the ETS rods to concrete. The effects of concrete compressive strength and embedded length on the bond performances of the ETS strengthened concrete blocks are also investigated. The results obtained from this study are compared and verified with the experimental data of the literature to confirm the effectiveness of the numerical and analytical investigations. This study provides insight into the mechanical performances of concrete blocks with the strengthening of ETS rods, builds the reliable FE models which can be used to predict the bond response of concrete members strengthened by the ETS technique, offers the rational, analytical formulas to evaluate the bond behavior between ETS bars and concrete.

Keywords— embedded through section (ETS); strengthening; bond behavior; finite element

I. INTRODUCTION

Till date, there were several experimental research on the shear strengthening of reinforced concrete (RC) members adopting the embedded through section (ETS) method [1-4]. O. Chaallal et al. [1] studied the performance of the ETS technique by comparing with the externally bonded (EB) and near surface-mounted (NSM) methods. The results in research of O. Chaallal et al. [1] indicated that the shear strength of the specimens without transverse steel strengthened by the ETS bars were significantly increased in comparison with the one attained using the EB and NSM techniques.

Furthermore, the studies of O. Chaallal et al. [1], A. Mofidi et al. [2], M. Breveglieri et al. [3] and M. Breveglieri et al. [4] concluded that the shear resistance would be enhanced by using the embedded through-section (ETS) bars. Moreover, the inclined ETS bars for strengthening were more effective than the vertical ETS bars. Also, those works showed that the ETS shear strengthening bars would convert the brittle shear failure into the ductile flexural failure with the yielding of the tension steel bars.

For the bond behavior in the ETS system, A. Godat et al. [5] and J. Barros [6] developed two-dimensional (2D) finite element analysis to model the fiber reinforced polymer (FRP) bar/ detailed interfacial response of the pull-out test using ETS technique. A. Godat et al. [5] used discrete truss elements oriented above and below the FRP bar connecting the two substrates to simulate the FRP bar/concrete interfacial behavior. Whereas, J. Barros et al. [6] mentioned the strategy for modeling the fracture mode II which were conducted in the FEM-based computer program with the smeared crack model, FEMIX. However, no study has ever presented the finite element (FE) modeling of concrete blocks strengthened by ETS bars nor the analytical solution of slip profiles in the ETS method.

In this study, the data of the previous research have been used to conduct the numerical and analytical investigation. The effects of concrete compressive strength and embedded length on the bond performances of the ETS strengthened concrete blocks are considered by employing the FE modeling in ANSYS software. Additionally, the analytical formulation of the slip profiles is also offered to assess the bond performance of ETS rods to concrete. The results obtained from this paper are compared and verified with the

experimental data of the literature to confirm the effectiveness of the numerical and analytical investigations.

II. MATERIAL AND METHOD

A. Experimental Data

The six specimens in the research of A. Godat et al. [7] are adopted to implement the numerical and analytical program of the current study. The various configurations, properties and tested results of the specimens in the research of A. Godat et al. [7] are summarized in Table 1. The cross-sectional dimensions of the concrete blocks were 190×190 mm [7]. More details of the tested specimens could be found in the study of A. Godat et al. [7]. In this study, the investigations into the effects of concrete strength and embedded length on the bond performances of the ETS strengthened concrete blocks are carried out. Also, the representative specimens in Table 1 are also employed to discuss the failure modes and the analytical computation in section III-B.

TABLE I
PROPERTIES OF TESTED SPECIMENS [7]

Specimens	f_c (MPa)	d_b (mm)	h_b (mm)	L (mm)	P (kN)
C1-1.50d-9.5B-15.0d	20.7	9.52	15	143	35.7
C2-1.50d-9.5B-15.0d	42.7	9.52	15	143	91.2
C2-1.50d-9.5S-5.0d	42.7	9.52	15	48	42.8
C2-1.50d-9.5S-10.0d	42.7	9.52	15	95	63.4
C2-1.50d-9.5S-20.0d	42.7	9.52	15	190	102.4
C2-1.50d-9.5S-25.0d	42.7	9.52	15	238	114.7

TABLE II
PROPERTIES OF MATERIAL AND CONCRETE SPECIMENS [7]

Specimens	E_c (MPa)	E_r (MPa)	Remarks
C1-1.50d-9.5B-15.0d	22000	120000	PSC
C2-1.50d-9.5B-15.0d	28500	155000	SS
C2-1.50d-9.5S-5.0d	28500	155000	SS
C2-1.50d-9.5S-10.0d	28500	155000	SS
C2-1.50d-9.5S-20.0d	28500	155000	SS
C2-1.50d-9.5S-25.0d	28500	155000	SS

Noting that C1/2-1.50d-9.5B-15.0d means concrete compressive strength C1/2 equals 20.7/42.7 MPa–Hole diameter (h_b) equals $1.5d_b$ –9.5B is the bar diameter (d_b)–Embedded length (L) equals $15d_b$. Moreover, P is the maximum applied load. Table 2 shows properties of specimens as the elastic modulus of concrete ($E_c = 3300\sqrt{f_c} + 6900$ (MPa)), and elastic modulus of ETS bars (E_r). Besides, types of FRP bar surface are described as PSC for pultrall sand coated and SS for Sika smooth.

B. Finite Element Program

In this section, the FE models using ANSYS 15.0 [8] of the six specimens in section II-A are built to investigate the

bond force-slip relations, and failure modes of concrete blocks strengthened with the ETS rods as the pull-out tests.

1) Element Types

SOLID65 is used for the nonlinear 3D modeling of concrete materials. The SOLID65 element is capable of cracking in tension and crushing in compression. The element is defined by eight nodes and at each node has three degrees of freedom that are the translations in the nodal x, y, and z directions. LINK180 element is assigned for the ETS strengthened bar. LINK180 is a uniaxial tension-compression element with three degrees of freedom at each node that the translations in the nodal x, y, and z directions [9]. The element of COMBIN39 with the bilinear relationship, which the knee point is at maximum bond stress and the stiffness in the remaining response is zero, between slip and bond force is employed to model the bond behavior of the ETS bars to concrete in the FE simulations.

2) Material Models

Previously, various constitutive models have been employed in the FE simulations of concrete components strengthened by ETS bars. The nonlinear elastic models, plasticity based models whether perfect plasticity models or elastic-plastic models were included in these models [7]. In this study, the model of Hognestad which is shown in the reference [11] is adopted to simulate the nonlinear response of concrete in compression.

The concrete behavior in tension according to the model of William and Warnke is recommended by ANSYS. The linear elasticity to the concrete tensile strength is used for concrete behavior in tension. Then, a step drop in the concrete tensile stress by 40% is the stress relaxation in tension. Moreover, the rest of model is represented as the curve which descends linearly to the zeros of the tensile stress were a strain value of 6 times larger than the strain value at the concrete's tensile strength [9], [11]. Besides, the ETS FRP bars are simulated as elastic-brittle materials till rupture.

C. Analytical Computation

1) The Existing Bond Models of FRP Bars to Concrete

E. Cosenza et al. [10] showed the three primary models of the bond behavior of FRP bars to concrete were the Eligehausen, Popov, and Bertero (BPE) model, modified BPE model, and Cosenza, Manfredi and Realfonzo (CMR) model.

In 1983, Eligehausen, Popov, and Bertero (BPE) model proposed a formula to determine the bond-slip relation in Fig. 1 and Eq. (1).

$$\frac{\tau}{\tau_1} = \left(\frac{s}{s_1} \right)^\alpha \quad (1)$$

Where $\tau_1 = \tau_m$ is a maximum bond strength, $s_1 = s_m$ is a corresponding slip with τ_m , α is a curve-fitting parameter less than or equals to 1.

$$\frac{\tau}{\tau_1} = 1 - p \left(\frac{s}{s_1} - 1 \right) \quad (2)$$

An alternative equation was proposed in the study of E. Cosenza et al. [11] via slightly modifying the BPE one. The

modified BPE model has shown the same ascending branch as the original one, a softening branch, having slope $p\tau_1/s_1$ from (s_1, τ_1) to (s_3, τ_3) which was given by Eq. (2) [11].

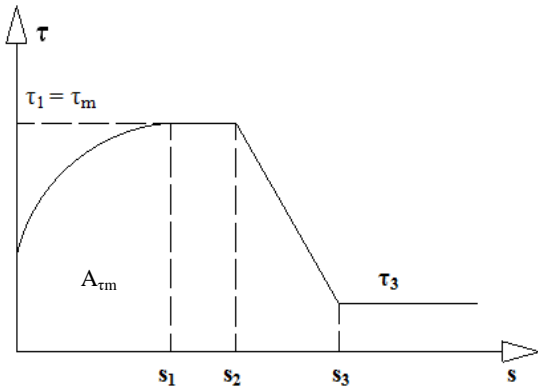


Fig. 1 Representative curve for BPE, modified BPE, and CMR models

Finally, CMR model was introduced in the research of E. Cosenza et al. [11]. In this model, the authors improved the ascending branch in BPE model by the following expression.

$$\frac{\tau}{\tau_m} = \left(1 - e^{-\frac{s}{s_r}}\right)^\beta \quad (3)$$

Where τ_m = peak bond stress; and s_r and β = parameters based on curve-fitting of the actual data [11].

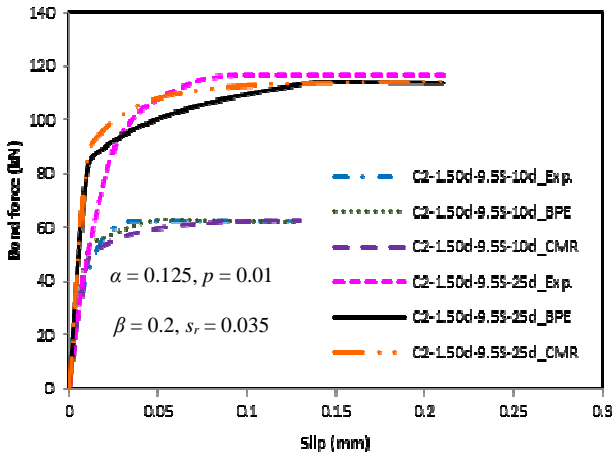


Fig. 2 A comparison of the existing bond models and experimental data

By considering the two specimens in section II-A, the representative results of the comparison between the analytical bond force-slip curves obtained from the use of the modified BPE model and the CMR model and the experimental data are shown in Fig. 2. It is evident from Fig. 2 that the CMR and modified BPE bond-slip laws perform the reasonable agreement with the tested results. A small discrepancy in the ascending branch in comparison with the experimental data is observed for the CMR curve rather than that of the modified BPE model. The presence of the fitting parameters in the models reduces the discrepancy in the computation. However, in the descending branch, the modified BPE model provides more conservative estimation than the descending branch using the CMR calculation. Therefore, the combination of the CMR and the modified

BPE laws for the ascending and descending branch, respectively, can be adopted to predict the bond force-slip relations of concrete members strengthened by ETS bars.

2) Mathematical Model of ETS Bond Response

The research on the bond behavior of FRP bars to concrete was based on the interaction directly of bar/concrete interface [12]. However, in the ETS technique, there were two interfacial interactions of ETS bar/adhesive material and concrete/adhesive material, this section, therefore, shows a new approach for bond behavior in the ETS technique. Figure 3 performs the block of concrete in tension; Fig. 4 describes the equilibrium forces in arbitrary section and the free body diagrams of concrete/adhesive material and ETS bar/adhesive material interfaces.

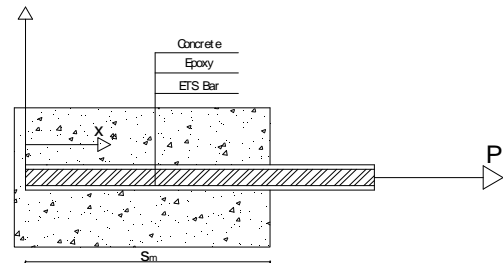


Fig. 3 The block of concrete using ETS technique in tension

From Fig. 4 the equilibrium equations can be obtained as follows.

$$\begin{aligned} dF_c(x) &= A_c d\sigma_c(x) = p_e \tau(x) dx \\ dF_e(x) &= A_e d\sigma_e(x) = -p_r \tau(x) dx \\ dF_r(x) &= A_r d\sigma_r(x) = p_r \tau(x) dx \end{aligned} \quad (4)$$

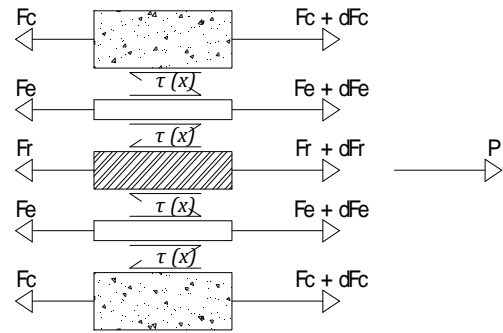


Fig. 4 The free body diagrams of the interfaces of materials

Where p_r, p_e is the perimeter of the bar and the adhesive material cover, and $\tau(x)$ is the bond stress, A_c, A_e, A_r are the cross-sectional area of concrete, adhesive materials cover, ETS bars, respectively. Additionally, $d\sigma_c(x), d\sigma_e(x), d\sigma_r(x)$ are the tensile stresses in the concrete, adhesive materials, and ETS rods at a distance x from the origin, respectively. Moreover, $dF_c(x), dF_e(x), dF_r(x)$ are the axial force in the concrete, adhesive material, ETS bars at a distance x from the origin, respectively.

The slip at the ETS bar–epoxy (adhesive material), epoxy–concrete interfaces and the relative slip between ETS bar–concrete are defined through Eq. (5).

$$\begin{aligned}
 s_1(x) &= u_r(x) - u_e(x) \\
 s_2(x) &= u_e(x) - u_c(x) \\
 s_3(x) &= s_1(x) + s_2(x) = u_r(x) - u_c(x)
 \end{aligned} \quad (5)$$

Where $s(x)$ is the slip, $u_r(x)$, $u_e(x)$, and $u_c(x)$ are the displacement along x -axis of the ETS bar, epoxy, and concrete, respectively. Besides, the uniaxial constitutive relationship for the linear elastic concrete, epoxy, and ETS bar elements are shown in Eq. (6).

$$\begin{aligned}
 F_c(x) &= E_c A_c \varepsilon_c(x) \\
 F_e(x) &= E_e A_e \varepsilon_e(x) \\
 F_r(x) &= E_r A_r \varepsilon_r(x)
 \end{aligned} \quad (6)$$

Where $F(x)$ is the axial force along the x -axis, $E_{c/e/r}$ is the elastic modulus of materials and $\varepsilon(x)$ is the axial strain at a distance x .

$$\begin{aligned}
 \frac{ds_3(x)}{dx} &= \varepsilon_r(x) - \varepsilon_c(x) \\
 \frac{d^2s_3(x)}{dx^2} &= \frac{d\varepsilon_r(x)}{dx} - \frac{d\varepsilon_c(x)}{dx}
 \end{aligned} \quad (7)$$

From Eq. (5), take the first and second derivatives of the third one obtained Eq. (7).

Substituting Eqs. (4)-(6) into the above equation, Eq. (7) can be written as Eq. (8).

$$\begin{aligned}
 \frac{d^2s_3(x)}{dx^2} &= \frac{dF_r(x)}{E_r A_r dx} - \frac{dF_c(x)}{E_c A_c dx} \\
 &= \frac{p_r \tau(x)}{E_r A_r} - \frac{p_e \tau(x)}{E_c A_c} = p_r \tau(x) \left(\frac{1}{E_r A_r} - \frac{p_e}{p_r E_c A_c} \right)
 \end{aligned} \quad (8)$$

Equation (8) performs the relationship between slip and bond stress functions, and this is a second order ordinary differential equation. By applying the numerical methods, Eq. (8) can be easily solved. However, this section shows merely a mathematical solution of Eq. (8) Using the BPE model in the analyses. Then, after substituting $\tau(x)$ in the model of Eligehausen, Popov, and Bertero (BPE model in Eq. (1)) into Eq. (8) leads to Eq. (9).

$$\frac{d^2s_3(x)}{dx^2} = \frac{p_r \tau_m}{s_m^\alpha} \left(\frac{1}{E_r A_r} - \frac{p_e}{p_r E_c A_c} \right) (s_3(x))^\alpha \quad (9)$$

The final solution of Eq. (9) is shown in Eq. (10).

$$s_3(x) = \left[\frac{K(1-\alpha)^2}{2(1+\alpha)} \right]^{\frac{1}{1-\alpha}} x^{\frac{2}{1-\alpha}} \quad (10)$$

$$\text{Where } K = \frac{p_r \tau_m}{s_m^\alpha} \left(\frac{1}{E_r A_r} - \frac{p_e}{p_r E_c A_c} \right)$$

Equation (10) indicates the nonlinear distribution of the slip along the embedded depth of ETS bars that the previous studies have stated.

A. Finite Element Investigation

The concrete blocks strengthened by carbon fiber reinforced polymer (CFRP) are simulated and investigated. The failure definition of the specimens in the FE analysis is either (1) the concrete tensile stress exceeding the ultimate tensile strength or (2) the stress in ETS bar reaching their tensile strength or (3) the slip between ETS bar and concrete exceeding the maximum slip. The predicted bond force-slip response, failure modes of the developed models are compared with the results obtained from the corresponding experimental data.

Figure 5 shows the bond force-slip curves of experimental and simulated results for the six specimens with the effects of concrete compressive strength and embedded length of the ETS bars. It is explicit that the FE results perform the good appraisal in comparison with the tested data, and a maximum deviation less than 10% not only in the bond force but also in the slip is easily obtained from Table 3 and Fig. 5. In addition, as shown in Table 3, the mean value of the ratio of the simulated bond forces to the tested results is 0.98 and the coefficient of variation is 3.67% of the mean. In general, the bond force-slip responses from the FE analysis fit well with the experimental results due to the interfacial element assumption between ETS bars and concrete in the FE model.

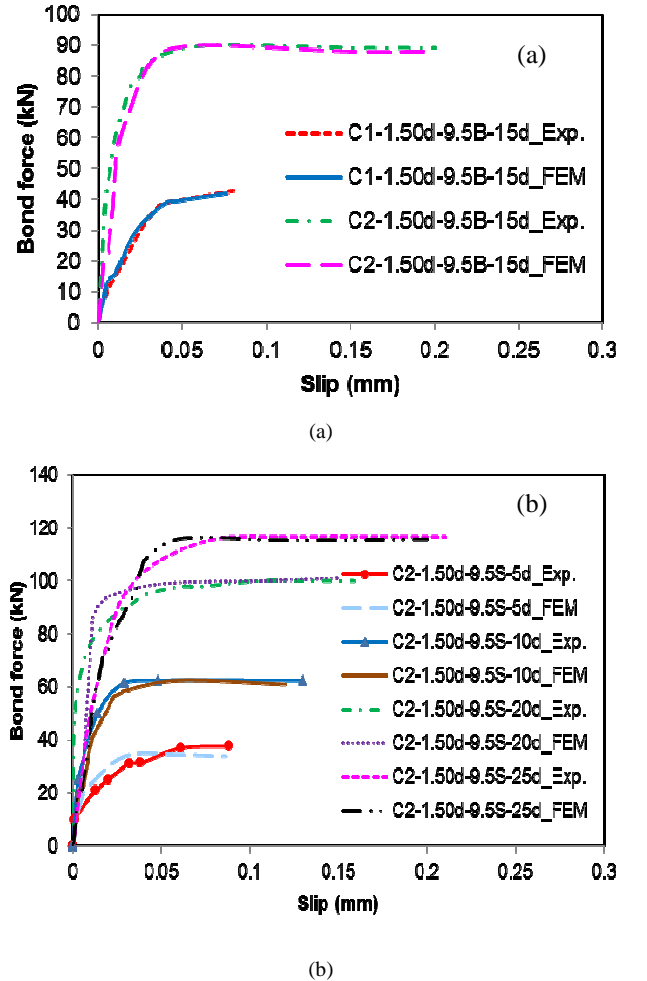


Fig. 5 Bond force and slip relationship: (a) effect of concrete strength and (b) effect of embedded length

TABLE III
EXPERIMENTAL AND NUMERICAL RESULTS FOR BOND FORCE CAPACITY AND
FAILURE MODE

Specimens	Bond force F (kN)			Failure mode	
	Tested	FEM	F_{FEM}/F_{Tested}	Tested	FEM
C1-1.50d-9.5B-15.0d	42.8	42.0	0.98	CS*	CS
C2-1.50d-9.5B-15.0d	89.3	88.0	0.99	BP*	BP
C2-1.50d-9.5S-5.0d	37.5	34.0	0.91	BP	BP
C2-1.50d-9.5S-10.0d	62.5	61.0	0.98	BP	BP
C2-1.50d-9.5S-20.0d	100.0	101.0	1.01	BP	BP
C2-1.50d-9.5S-25.0d	116.7	116.0	0.99	BR*	BR

*CS, BP, and BR are corresponding failure modes of the specimens by concrete splitting, bar pull-out (bar surface) and bar rupture, respectively.

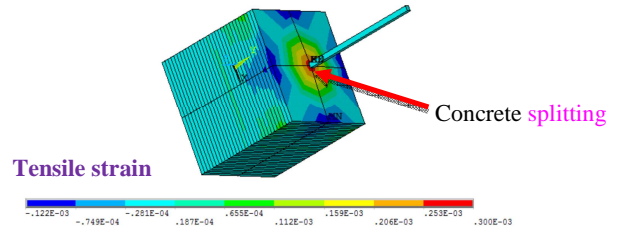
The effect of concrete strength on the bond performance of concrete blocks strengthened by ETS bars is indicated in Fig. 5(a). By increasing concrete compressive strength, from C1 (20.7 MPa) to C2 (42.7 MPa), the bond resistance increases with 1.6 times in the bond force. For the influence of embedded length of ETS bars, Fig. 5(b) performs that the bond resistance enhances with the increase of embedded depth of ETS rods from $5d_b$ to $25d_b$ (d_b is bar diameter of ETS rod). The numerical results in Fig. 5(b) demonstrate that the increase in the embedded bond length for specimens C2-1.5d-9.5S-5d to C2-1.5d-9.5S-25d is five times, while the corresponding enhancement in the bond force is 2.5 times.

To discuss the failure modes of concrete blocks strengthened by ETS rods, the two representative specimens in the effect of concrete strength are deeply considered. By testing, the failure modes of the specimens C1-1.50d-9.5B-15d and C2-1.50d-9.5B-15d were the concrete splitting and the bar surface, respectively, which have been shown in the experimental program of A. Godat et al. [7].

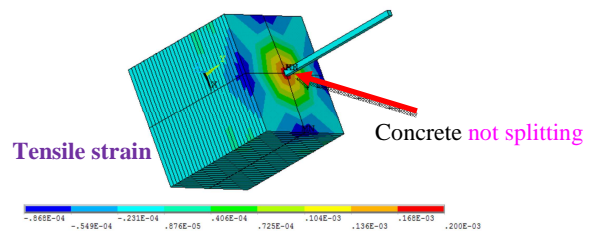
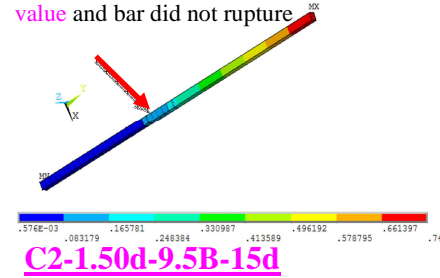
The failure above modes is completely matched to the simulation results in Fig. 6. For C1-1.50d-9.5B-15d, at ultimate load concrete strain exceeds the tensile strain, slip and ETS bar stress do not reach to the allowable values. Therefore, the specimen C1-1.50d-9.5B-15d failed in concrete splitting. For C2-1.50d-9.5B-15d, the slip exceeds the maximum value, the concrete strain and ETS rod stress do not reach to the ultimate values. Thus, the failure mode of C2-1.50d-9.5B-15d involved in the ETS bar and adhesive interface. It can be explained that the concrete matrix structure of high strength concrete is stiffer and more stable than that of low strength concrete. Furthermore, Table 3 also shows a comparison in the failure modes of the investigated specimens, the failure mode of the specimens considered by the FE simulation is the same as the failure mode of the members tested by A. Godat et al. [7], which is determined by either concrete splitting or bar pull-out (bar surface) or bar rupture.

In concluding, the FE method is a useful tool to accurately predict various features, including the bond force-slip relationship, stress/strain responses of concrete and ETS bars, and failure modes of concrete members strengthened by ETS bars.

C1-1.50d-9.5B-15d



Slip did not reach maximum value and bar did not rupture



Slip reached maximum value and bar did not rupture

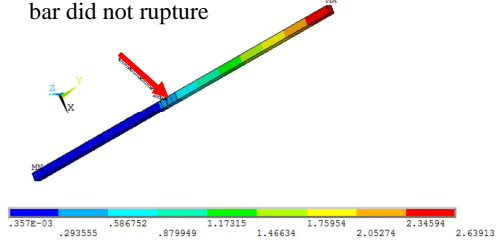


Fig. 6 Failure modes of the two representative specimens C1-1.50d-9.5B-15d and C2-1.50d-9.5B-15d

B. Analytical Investigation

By using the mathematical formulation in section II-C-2, the slip profiles of the two specimens C2-1.5d-9.5S-10d and C2-1.5d-9.5S-25d, which represent for the cases of short embedded length and long embedded length, respectively, are investigated. The analytical results of the slip distributions along the ETS bars are compared with the FE results and the simulated data of the previous study.

Figure 7 shows the slip distributions along the embedded length of the specimens C2-1.5d-9.5S-10d and C2-1.5d-9.5S-25d. The FE results fit well with the numerical study attained by A. Godat et al. [5] in the cases of the short and long embedded length of the two concrete blocks. On the

other hand, the mathematical solution offers a good agreement with the FE result and the previous data in the case of the short embedded length. Whereas, a significant discrepancy between the analytical and numerical results is observed in the case of the long embedded length. The main reason for this difference is the influence of the confinement action of the concrete block with the extended embedded depth of ETS rod, which was assigned in the numerical analysis using the bar/concrete interfacial element. However, the confinement action was not considered in the analytical solution by adopting the BPE model as Eq. (9).

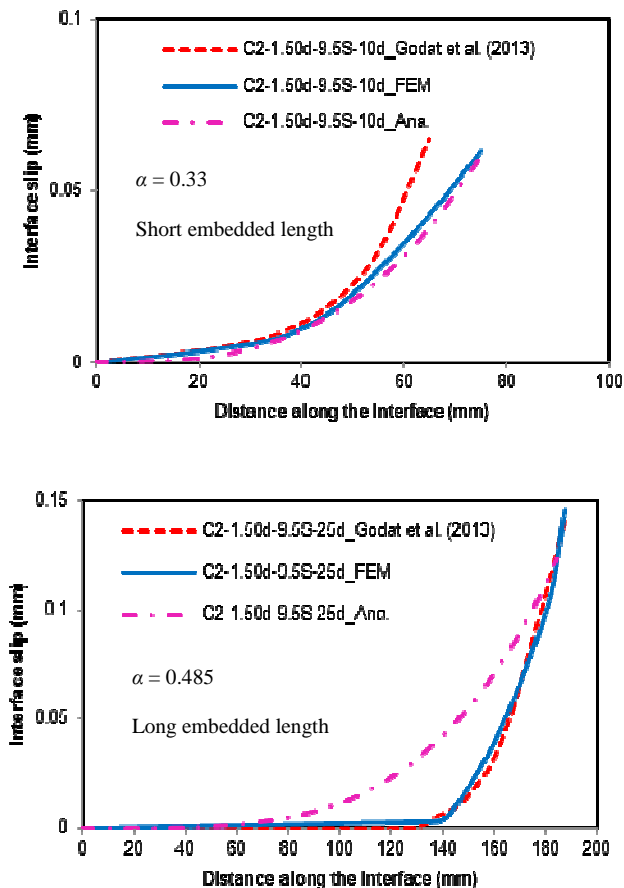


Fig. 7 Slip profiles along the embedded length

The mathematical solution presents a simple application to predict the slip behaviors along the embedded depth of ETS rods. However, the substitution of the equation of the BPE bond-slip law into the governing equation (Eq. (8)) leads to the analytical results is not good enough to determine the slip profiles. Therefore, the alternative solutions as the substitution of the CMR's formula into Eq. (8) alternatively, the numerical methods for solving Eq. (8) are expected in the future research. Besides, to confirm the numerical and analytical results, the authors believe that an experimental program is necessary to investigate the slip responses along the embedded length of concrete blocks strengthened by ETS bars.

IV. CONCLUSIONS

A numerical and analytical study was merely carried out with the objective of understanding the bond behavior between the ETS bars and concrete. Based on the results of the analyses, conclusions could be drawn:

- The reliable FE models were built to obtain the right predictions for the bond response of the concrete members strengthened by ETS bars with reasonable accuracy in comparison with the tested results;
- The bilinear relationship could be performed for the bond force-slip behavior of the strengthened concrete components using the ETS method;
- Enhancing concrete strength and embedded length, the bond resistance increases. Additionally, the changes in the failure modes were also observed in these effects;
- The existing bond models were acceptable to describe the bond force and slip relationship. In the current study, the combination of the ascending branch in the CMR model and the descending branch in the modified BPE model was suggested to perform the bond response of the strengthened concrete specimens by applying the ETS method;
- A governing equation of the bond behavior between ETS bars and concrete was established. Then, the mathematical solution by adopting the BPE model in the analysis was also implemented. By comparing with the numerical results in the FE simulation and previous study, the analytical investigation agreed well and indicated that the slip profile along the embedded depth is a nonlinear distribution;
- Also, the confinement action played a significant role in the bond performance of the strengthened concrete blocks using the ETS technique. Thus, the additional research on this problem is needed;
- The authors were planning the numerical and experimental studies on the topics related to the bond behavior as well as the structural response of concrete members strengthened by ETS bars.

ACKNOWLEDGMENT

This study was financially supported by the ASEAN University Network/Southeast Asia Engineering Education Development Network-AUN/SEED-Net.

REFERENCES

- [1] O. Chaallal, A. Mofidi, B. Benmokrane, and K. Neale, "Embedded through-section FRP rod method for shear strengthening of RC beams: Performance and comparison with existing techniques," *Journal of Composites for Construction*, vol. 15, pp. 374-383, Mar. 2011.
- [2] A. Mofidi, O. Chaallal, B. Benmokrane, and K. Neale, "Experimental tests and design model for RC beams strengthened in shear using the embedded through-section FRP method," *Journal of Composites for Construction*, vol. 16, pp. 540-550, May 2012.
- [3] M. Breveglieri, A. Aprile, and J. A. O. Barros, "Shear strengthening of reinforced concrete beams strengthened using embedded through section steel bars," *Engineering Structures*, vol. 81, pp. 76-87, Oct. 2014.
- [4] M. Breveglieri, A. Aprile, and J. A. O. Barros, "Embedded through-section shear strengthening technique using steel and CFRP bars in RC beams of different percentage of existing stirrups," *Composite Structures*, vol. 126, pp. 101-113, Feb. 2015.

- [5] A. Godat, O. Chaallal, and K. Neale, "Nonlinear finite element models for the embedded through-section FRP shear-strengthening method," *Computers & Structures*, vol. 119, pp. 12-22, Jan. 2013.
- [6] J. Barros, M. Breveglieri, A. V. Gouveia, G. Dalfre, and A. Aprile, "Model to simulate the behavior of RC beam shear strengthened by ETS bars," [Online]. Available: <http://hdl.handle.net/1822/26277>, 2013.
- [7] A. Godat, A. L'Hady, O. Chaallal, and K. Neale, "Bond behavior of the ETS FRP bar shear - strengthening method," *Journal of Composites for Construction*, vol. 16, pp. 529-539, May 2012.
- [8] ANSYS – Release Version 15.0, "A finite element computer software and user manual for nonlinear structural analysis," Canonsburg, USA, 2013.
- [9] R. A. Hawileh, "Finite element modeling of reinforced concrete beams with a hybrid combination of steel and aramid reinforcement," *Materials & Design*, vol. 65, pp. 831-839, Oct. 2015.
- [10] E. Cosenza, G. Manfredi, and R. Realfonzo, "Behavior and modeling of the bond of FRP rebars to concrete," *Journal of Composites for Construction*, vol. 1, pp. 40-51, Feb. 1997.
- [11] L. V. H. Bui, B. Stitmannathum, and T. Ueda, "Mechanical performances of concrete beams with the hybrid usage of steel and FRP tension reinforcement," *Computers and Concrete*, vol. 20, pp. 391-407, Oct. 2017.
- [12] M. B. Munov, "Study on the behaviour of FRP and concrete," Ph.D. thesis, the University of Girona, 2010. [Online]. Available: <http://hdl.handle.net/10803/7771>.